A Novel Computational Thermal-Visual Imaging System for Automatic Cornea Temperature Measurement and Tracking

Ehsan Zare Bidaki, University of Waterloo, ON, Canada
Alexander Wong, University of Waterloo, ON, Canada
Paul Murphy, University of Waterloo, ON, Canada
Email: {ehsanzb, alexander.wong, paul.murphy}@uwaterloo.ca

Abstract

Ocular surface temperature (OST) is affected by changes in the physiology of the eye caused by normal homeostasis, environmental changes, or systemic and local disease. OST can help a physician to diagnose eye disease with improved accuracy and provide useful information for eye research. This paper presents a novel system including novel hardware design and novel algorithms to measure and track OST from the cornea automatically over any period of time. The system uses an IR camera and a visible light camera to capture synchronous thermal and visible videos, respectively, from the eye surface. The frames for the two video sequences are then registered and the cornea was segmented using a semantic segmentation method. At the final step, the corneal area was localized on the registered thermal frames to extract temperature information. The mean square error for the registration was 5.03 ±1.82 and the mean Intersection over Union (IoU) was 94.6%, representing the accuracy of corneal segmentation. A system for measuring and tracking eye surface temperature over time was developed. The system is able to localise the cornea on both visible and thermal images and report temperature profiles of the cornea over the period of measurement. Experimental results shows that the whole system can work as a tool for measuring and tracking OST over time.

Fig. 2: Designed Dual camera System

1 Introduction

IR thermography has been used as a non-invasive method of ocular surface temperature measurement to assist clinicians in diagnosing several ocular diseases [1–4]. A precise IR thermogram can help physicians to diagnose eye diseases with much improved accuracy and opens new avenues in research. Figure 1 shows an example of a visible-range image and corresponding thermal image from the ocular surface.

Fig. 1: Sample thermal and visible-range images of the eye

Current methods employ either a single camera or dual camera arrangement. A single camera uses an IR camera, but localisation of the cornea as the area of interest is limited due to the lack of thermal distinction across the ocular surface. Dual camera systems attempt to use a visual camera, in combination with the thermal camera to assist in locating specific areas of interest on the ocular surface. However, these systems do not synchronise their video streams from each camera and are thus unable to accurately locate and track the corneal area in the thermal image during a measurement sequence. This limits the available options for tracking changes in temperature over time, as well as limiting the possible analysis of OST across the cornea during the measurement period. Previous systems are also unable to detect and remove artefacts in the OST data due to eye movement and eyelid closure. Lastly, they are not fully automatic. In this paper, we propose a novel system for imaging the eye and gathering useful OST data across the full eye surface that incorporates a reliable and precise method to detect the corneal boundary on the thermal images, and can track the temperature across all parts of the cornea over time.

Mapstone [5] was the first person to use a non-contact method to measure OST. A bolometer (thermal detector) was used to measure the radiation from the surface of the eye. In the 1970s, the emergence of new cameras with better sensitivity and magnification provided an improved facility to capture temperature data from the ocular surface. These early cameras incorporated some form of detector and required liquid nitrogen for cooling of the detector to enable detection of IR radiation. With the subsequent development of semi-conductor CCDs, the detectors have been revolutionised in their level of sensitivity, speed of operation, and they can work at room temperature [6].

IR thermography provides an opportunity to measure the temperature of the whole cornea, or a specific area, such as a circle around the center, or limbus. Many studies have been undertaken on the use of IR thermography and OST[1]. Published studies reporting on the measurement of OST describe varying methods for analysis of the captured IR thermography image [7].

The methods for estimation of the OST can be grouped into two categories: single camera and dual camera system. In the single camera systems, a thermal camera was used to measure the OST. Generally, these methods are divided into three categories: manual, semi-automatic, and automatic methods.

In the manual methods, each image produced was analysed by the user manually selecting a single point, multiple points, or drawing a circle/square as the area of interest. For example Efron et al. (1989) [8] measured OST at 11 points on the surface of the cornea, Murphy et al. (1999) [9] used five boxes placed along a horizontal line centered on the cornea, and Chiang et al. (2006) and Ng et al.(2008) [10, 11] placed an encircled area (4.4mm diameter) on the center of the cornea to extract OST. The manual methods, while simple in their performance, have deficiencies arising either from the camera technology itself – low thermal and temporal accuracy, varying degrees of invasiveness – or from the limitations of data analysis – they are non-automatic and require much post-processing.

By improving both the thermal camera capabilities and quality, researchers have tried to improve their measurement results by implementing image processing algorithms. For example, Acharya et al. (2009) [12] and Matteoli et al. (2018) [13] each proposed a semi-automated method to acquire OST. Their method did not depend on ocular geometry and could be applied to compare OST between the

left and right eyes, or between different groups of people. Tan et al. (2009) [14] proposed a fully automated method to measure OST. Using their method, which included a snake algorithm and target tracing function, the eye was localised on the image, and the eyelash effects removed from the image. Finally, a circle was drawn in the center of the eye automatically to achieve cornea temperature data. However, their algorithm could not omit the influence of the eyelash completely and the accuracy of segmentation was not satisfactory.

The manual, semi-automatic, and fully automatic methods described thus far depend on a single camera system. They are not suitable for OST measurement and tracking either because they are manual or have low accuracy in locating the corneal ROI. To solve this problem, some groups have used a dual camera system to improve the accuracy of the segmentation.

Kamao et al. (2011) [15] used a visible camera embedded in a thermal camera system to measure OST in DED patients in a semi-automatic method. In their system, the ROI was segmented from the images manually and the extracted data analysed. However, the method was not synchronous and required a lot of user input to extract the data. Su et al. (2014) [16] used a different dual camera system to analyse tear film break-up patterns. To permit simultaneous imaging of the thermal and visible cameras, a germanium beam-splitter was used to transmit IR light and reflect visible light. The thermal camera and beam-splitter were installed in front of the patient's eye and the visible camera was located alongside. The system was an improvement in terms of synchronisation over the previous method. However, user input was still needed to analyse the tear-film patterns. In 2015, Li et al. [17] used a different camera installation topology by installing the cameras within -15° and +15° off-axis from the geometric center of the cornea to record two video files from the ocular surface. The tear film break-up area was then estimated by an experienced user looking at the thermal and visible-range videos simultaneously. Kricancic et al. (2017) [18] demonstrated another camera installation topology to monitor OST change on the surface of the eye. They used a germanium filter in a fixed position in front of the patient's eye. The system was used to monitor OST change in the contact lens wearer. However, their method still required manual input of the user.

A dual camera system is a simple method that permits location of the corneal and eye contour area in the thermal image. All of the reported dual camera system methods tried to have the best camera installation and adjustment in order to have the same image from the eye surface. However, adjusting two cameras to have the same field of view from a scene is difficult, and the resultant images from the two different sources are not identical. Images from different sensors can be affected by many factors, such as sensor pixel size, image resolution, lens distortion, environment light, distance, angle of photography, and sensor type. Therefore, working only on camera installation alignment will not yield data extraction with a high spatial accuracy. To improve the accuracy of cornea localisation on the thermal images, the images should be processed after finding the best camera alignment. To conclude, most of the described methods estimate the corneal location based on eyelid position and cannot track the corneal area during eye movement, blinking, or eccentric gaze. This occurs because the eye thermograph lacks a corneal boundary, which is clearly visible in colour images. Also, other methods, which may have more accuracy, need user input to extract the data. All of the above methods made a good contribution to OST measurement, but there are some weaknesses with each method. None of the described methods are able to localise the cornea with high accuracy and track it over time. Also, the methods cannot detect and remove blink artefacts from the image sequences. Hence, a system was designed and developed to overcome with these problems.

2 Material and Methods

2.1 Physical System

The best system for measuring and tracking OST over time is to use a dual camera system consisting of a thermal and a visible camera. A Teledyne FLIR IR A655sc thermal camera (Teledyne FLIR LLC, Wilsonville, OR, USA) with a close-up lens was chosen for this project. The camera was able to capture images at 172 mm working distance and 5.8x magnifying factor. FLIR BFS 51S5C-C machine vision camera (Teledyne FLIR LLC, Wilsonville, OR, USA) with Fujinon HF12.5SA-1 close-up lens (Fujifilm Corp, Tokyo, Japan) was selected for the visible camera. The FOV for the visible camera was adjusted to match the FOV of the thermal camera. The same image size (640 x 480 pixels) was chosen for the thermal and visible cameras with frame rate of 25 fps. Figure 2 shows the camera set-up for the system.

2.2 Algorithm design and development

The first step was to develop an algorithm to manage the camera system and acquire synchronous frames from both cameras. The developed algorithm had the ability to record individual image sequences from each camera synchronously. The synchronisation of the cameras were determined accurate by comparing timestamps of the frames, and the video frames comparison side by side. After recording and normalising the video files, each pixel on the visible video frame now has a matching pixel in the corresponding thermal video frame. However, because of the misalignment of the two cameras, there are translational and rotational errors between the two images and the images do not overlap precisely. In later steps of system development, the visible camera image will be used to localise the cornea, and then the corneal localisation from the visible camera will be used to identify the corneal area in the thermal image. To do that, the coordinates of the cornea will be identified in the visible-range image and then those coordinates will be used as the location of the cornea in the thermal image. For this to work, the video frames from each camera must be registered. To do the video registration, the corresponding frames should be registered on each other. Therefore, a set of corresponding control points are required for each pair of the corresponding frames. The first set of corresponding control points were manually selected on the images. Then, the points were localized on the frames automatically using the Lucas and Kanade (LK) [19] optical flow algorithm. After point localization, the corresponding video frames were registered using the Affine image registration technique [20]. To extract the OST values for the cornea from each thermal video frame, the corneal area must be localised on the thermal image of the eye. However, thermal image formation is based on the temperature distribution across the ocular surface and there is no clear boundary that separates the cornea from the conjunctiva in the thermal images. The previously reported steps of video registration for the dual camera system have produced an aligned visible and thermal image. Therefore, the cornea can be localised in the thermal image by first using the visible-range image to identify and segment the cornea, and then using this segmented area as a mask over the thermal image to locate the cornea. The limits of the cornea on the visible-range image are best found by identifying the underlying iris, since the iris provides a strong contrasting signal to the visual contrast of the neighboring sclera. Semantic segmentation was used to segment cornea in the visible-range images and localise it in the corresponding thermal images.

3 Results and Discussion

Two synchronous videos, visible-range and thermal, were recorded from the eye surface. The cameras were adjusted to 25 fps and 250 frames were recorded for 10 seconds. for the first step, the LK algorithm used to localise control points on each frame of the video files. Table 1 shows the calculated error.

Table 1: Calculated optical flow algorithm error

Video File	Calculated Error (MSE ± SD)
Visible video	5.43 ±2.01 pixels = 5.43 * 0.09 mm
Thermal video	6.81 ±2.32 pixels = 6.81 * 0.09 mm

After localising the control points in each frame, the video files were registered using the point coordinates of the control points on the visible and thermal frames, using the Affine image registration algorithm. Any misplacement of the points in the registration process is known as the registration error. A common measure of overall point misalignment is the root-mean square (RMS) error, which is also called the fiducial registration error (FRE). Mean FRE ± SD= 5.03 ±1.82 pixels, gained over 250 frames.

Semantic segmentation was used in this project to segment cornea from the images. For the training and testing the network, a

total of 160 images of the eyes of 10 subjects were captured to produce the dataset used in this project. Resnet-PSPNet was chosen for cornea segmentation, with a mean IOU accuracy equal to 94.%. After localising the cornea, the blink frames were removed from the video files by assuming non-detected cornea frames representing a blink.

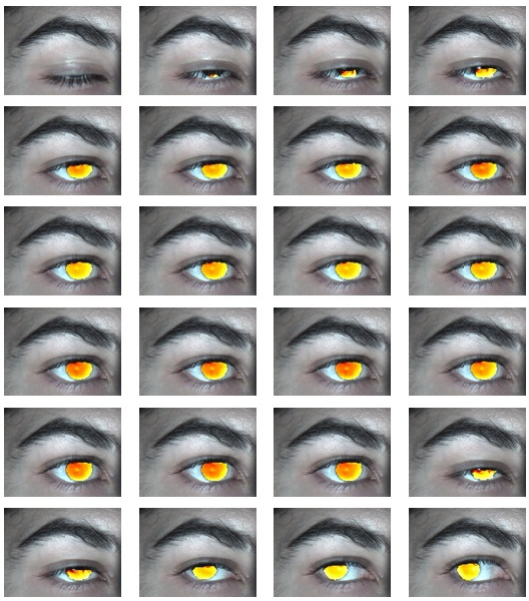

Fig. 3: Sample output of the whole system

The system has been shown to be able to register video files, to segment the cornea and to deal with eye movement artefacts. Figure 3 shows a sequence of registered video frames after the whole algorithm implementation. The figure shows extracted consecutive frames from the video file after a blink. The temperature profile is mapped on the corneal area from the thermal image. The temperature changes are demonstrated by obtained colour change in the images. There is no temperature mapped on the blink frames, which means there is no cornea detected in the frame. The last row of the figure demonstrates the eye tracking by the proposed method. When the cornea was moved in the frames, the ROI is segmented correctly, and the temperature profile is mapped on the ROI.

4 Conclusion

OST measurement provides useful information about ocular surface health. For example, knowledge of the OST can help a physician to diagnose some eye diseases with much improved accuracy. It can also be used for a better understanding of tear film quality by looking at changes in OST associated with tear film break-up. However, current methods for assessing OST clinically are severely limited. No commercial systems for assessing OST are available and researchers have instead relied on customised instruments. Of the instruments available, all are designed with either one camera (thermal) or two cameras (one thermal and one visible). The dual camera systems are designed to use the visible camera to help overcome the inherent lack of spatial resolution across the thermal image that makes precise identification of the corneal boundary very difficult.

This paper reports on the development of a novel system and method for imaging, segmenting, and temporal and spatial tracking of visible and IR images of the ocular surface and eye adnexa. The developed system has the ability to locate the corneal area in the thermogram and consistently measure from the same location on the ocular surface by tracking and compensating for any head or eye movements. It can remove artefacts like blinking and eye movement from the recorded video files and track reliable OST changes over time. For the first time, a complete system for imaging the ocular surface, synchronising video sequences, segmenting the cornea, and extracting ocular surface temperature (OST) data from the eye has been developed. The calculated accuracy in each step shows that the system has the potential to be used in OST measurement and tracking.

5 Acknowledgement

We acknowledge the support of the Natural Sciences and Engineering Research Council of Canada (NSERC).

References

[1] A. M. Shah and A. Galor, “Impact of ocular surface temperature on tear characteristics: current insights,” *Clinical Optometry*, vol. 13, p. 51, 2021.

[2] M. Rolando and M. Zierhut, “The ocular surface and tear film and their dysfunction in dry eye disease,” *Surv. Ophthalmol*, vol. 45, pp. S203–S210, 2001.

[3] H. Naidorf-Rosenblatt, D. Landau-Part, J. Moisseiev, A. Alhalel, R. Huna-Baron, A. Skaat, S. Pilus, L. Levi, and A. Leshno, “Ocular surface temperature differences in retinal vascular diseases,” *Retina*, vol. 42, no. 1, pp. 152–158, 2022.

[4] T. Rosenstock, P. Chart, and J. Hurwitz, “Inflammation of the lacrimal drainage system-assessment by thermography,” *Ophthalmic Surg*, vol. 14, no. 3, pp. 229–237, 1983.

[5] R. Mapstone, “Determinants of corneal temperature.” *Br J Ophthalmol*, vol. 52, no. 10, p. 729, 1968.

[6] C. Purslow and J. S. Wolffsohn, “Ocular surface temperature: a review,” *Eye & Contact Lens*, vol. 31, no. 3, pp. 117–123, 2005.

[7] J.-H. Tan, E. Ng, U. R. Acharya, and C. Chee, “Infrared thermography on ocular surface temperature: a review,” *Infrared physics & technology*, vol. 52, no. 4, pp. 97–108, 2009.

[8] N. Efron, G. Young, and N. A. Brennan, “Ocular surface temperature.” *Current eye research*, vol. 8, no. 9, pp. 901–906, 1989.

[9] P. J. Murphy, P. B. Morgan, S. Patel, and J. Marshall, “Corneal surface temperature change as the mode of stimulation of the non-contact corneal aesthesiometer.” *Cornea*, vol. 18, no. 3, pp. 333–342, 1999.

[10] H. K. Chiang, C. Y. Chen, H. Y. Cheng, K.-H. Chen, and D. O. Chang, “Development of infrared thermal imager for dry eye diagnosis,” in *Infrared and Photoelectronic Imagers and Detector Devices II*, vol. 6294. SPIE, 2006, pp. 36–43.

[11] E. Ng, J. Tan, E. Ooi, C. Chee, and U. Acharya, “Variations of ocular surface temperature with different age groups,” *Image Modeling of Human Eye, Artech House*, 2008.

[12] E. Ng, G. C. Yee, T. J. Hua, M. Kagathi *et al.*, “Analysis of normal human eye with different age groups using infrared images,” *Journal of medical systems*, vol. 33, no. 3, pp. 207–213, 2009.

[13] S. Matteoli, D. Coppini, and A. Corvi, “A novel image processing procedure for thermographic image analysis,” *Medical & Biological Engineering & Computing*, vol. 56, no. 10, pp. 1747–1756, 2018.

[14] J.-H. Tan, E. Y. Ng, and R. Acharya U, “Automated detection of eye and cornea on infrared thermogram using snake and target tracing function coupled with genetic algorithm,” *Quantitative InfraRed Thermography Journal*, vol. 6, no. 1, pp. 21–36, 2009.

[15] T. Kamao, M. Yamaguchi, S. Kawasaki, S. Mizoue, A. Shiraishi, and Y. Ohashi, “Screening for dry eye with newly developed ocular surface thermographer,” *Am. J. Ophthalmol*, vol. 151, no. 5, pp. 782–791, 2011.

[16] T.-Y. Su, S.-W. Chang, C.-J. Yang, and H. K. Chiang, “Direct observation and validation of fluorescein tear film break-up patterns by using a dual thermal-fluorescent imaging system,” *Biomedical optics express*, vol. 5, no. 8, pp. 2614–2619, 2014.

[17] W. Li, A. D. Graham, S. Selvin, and M. C. Lin, “Ocular surface cooling corresponds to tear film thinning and breakup,” *Optom Vis Sci*, vol. 92, no. 9, pp. e248–e256, 2015.

[18] H. Kricancic, H. McNeill, M. Titze, D. Alonso-Caneiro, and M. J. Collins, “Instrument for simultaneous assessment of fluorescein and thermal dynamics of the tear film,” in *2017 ARVO ASIA Meeting*, 2017.

[19] B. D. Lucas, T. Kanade *et al.*, *An iterative image registration technique with an application to stereo vision*. Vancouver, 1981, vol. 81.

[20] R. Hartley and A. Zisserman, *Multiple view geometry in computer vision*. Cambridge University Press, 2003.